Fenofibrate improves the impaired endothelial progenitor cell function through inhibiting eNOS uncoupling in diabetic mice

Running title: fenofibrate and eNOS uncoupling

Ting Zhao[2], Ya-Ping Deng[3], Min Ni[2], Ji-Kuai Chen[2], Zhang-Peng Li[2], Dong-Jie Li[1], Fu-Ming Shen[1,2]

[1]*Department of Pharmacy, Shanghai Tenth People's Hospital, Tongji University, Shanghai, China*
[2]*Department of Pharmacology, School of Pharmacy, Second Military Medical University, Shanghai, China*
[3]*Department of Pharmacy, Zhejiang Xiaoshan Hospital, Hangzhou, Zhejiang, China*

- TZ and YPD designed and conducted the experiments, analyzed the data, and wrote the manuscript.
- MN, JKC, ZPL and DJL conducted the experiments.
- FMS designed the experiments and wrote the manuscript.

The first two authors contributed equally.

Address requests for reprints to: Fu-Ming Shen, MD, PhD, Director, Department of Pharmacy, Shanghai Tenth People's Hospital, Tongji University, Shanghai 200072, China.

Tel: 86-21-66307668

E-mail: fumingshen@tongji.edu.cn and fumingshen@hotmail.com

This article has been accepted for publication and undergone full peer review but has not been through the copyediting, typesetting, pagination and proofreading process, which may lead to differences between this version and the Version of Record. Please cite this article as doi: 10.1111/bph.13054

Abstract

BACKGROUND AND PURPOSE

Fenofibrate decreases the risk of diabetic complications, including reducing the risk for minor amputations, but the mechanism(s) of action remains unclear. This study tested the hypothesis that fenofibrate could accelerate wound healing by improving the impaired endothelial progenitor cells (EPCs) function *via* inhibiting eNOS uncoupling in streptozotocin-induced diabetic mice.

EXPERIMENTAL APPROACH

Role of fenofibrate (100 mg/kg/d×14d, *i.g.*) in diabetic mice was assessed. Wound closure was evaluated by wound area and CD31 stained capillaries. EPCs function was determined by migration and tube formation assays. eNOS uncoupling of EPCs was assessed by measuring total, phosphorylated, monomer and dimer eNOS expression, and intracellular NO, O_2^-, BH_4, GTPCH1 and DHFR levels. *In vitro*, action of fenofibrate in high glucose induced EPCs dysfunction was assessed.

KEY RESULTS

Fenofibrate treatment obviously accelerated wound healing and stimulated angiogenesis in diabetic mice. EPCs function was significantly decreased in diabetic mice, fenofibrate treatment recovered the impaired EPCs capacities of both migration and tube formation. Furthermore, fenofibrate significantly enhanced eNOS phosphorylation and raised eNOS dimer-to-monomer ratio, increased NO production and decreased O_2^- level in EPCs of diabetic mice. Besides, fenofibrate restored the intracellular BH_4 and GTPCH1 in EPCs of diabetic mice. *In vitro*, fenofibrate dose dependently improved high glucose-impaired EPCs function.

CONCLUSION AND IMPLICATIONS

Fenofibrate could accelerate wound healing in diabetic mice, which at least in part was mediated by improving the impaired EPCs function through inhibiting eNOS uncoupling.

Abbreviations

EPCs, endothelial progenitor cells; BH_4, tetrahydrobiopterin**;** GTPCH1, guanosine triphosphate cyclohydrolase-1; DHFR, dihydrofolate reductase

Introduction

Micro- and macro-vascular complications are major causes of disability and death in patients with diabetes mellitus (Kar P and Holt, 2008). Endothelial dysfunction, resulted from reduced bioavailability of nitric oxide (NO) due to acceleration of NO degradation by reactive oxygen species (ROS), plays a key role in the pathogenesis of diabetic micro-vascular complications. In addition, during the process of NO degradation superoxide anion (O_2^-) is over-generated, which in turn inactivates NO (Fleissner and Thum, 2011; Förstermann and Li, 2011). Although hyperglycemia, insulin resistance, hyperinsulinemia and dyslipidemia independently contribute to endothelial dysfunction *via* several distinct mechanisms (Kim *et al.*, 2006), increased oxidative stress seems to be the first alteration triggering several others (Tousoulis *et al*., 2013; Wang *et al*., 2014).

Endothelial progenitor cells (EPCs) is a group of multi-progenitor cells, which has features of self-renewal, increases and differentiates into endothelial cells (Asahara *et al*., 1997). Studies have shown that EPCs plays a critical role in vascular endothelium integrity, in vascular repair and regeneration (Inoue *et al*., 2011, Liu *et al*., 2011). Accumulating evidences suggest that circulating EPCs, derived from the bone marrow, contribute to endothelial recovery (Lee and Yoon, 2013). Decreased levels of circulating EPCs are correlated with increased risk for coronary artery disease (Briguori *et al*., 2010). Endothelial nitric oxide synthase (eNOS), which could regulate mobilization and function of EPCs, is uncoupled in diabetes mellitus due to oxidant stress (Fleissner and Thum, 2011; Hamed *et al*., 2011), and uncoupling of the eNOS in blood vessels of diabetic patients lead to excessive O_2^- production and diminishes NO availability (Cassuto *et al*., 2014; Thum *et al*., 2007).

Peroxisome proliferator-activated receptor α (PPARα) is a ligand-inducible transcription factor that belongs to the nuclear-hormone-receptor family. PPARα agonist fenofibrate is mainly used in the treatment of dyslipidemia. The ACCORD (Action to Control Cardiovascular Risk in Diabetes) study supports that the addition of fenofibrate to a statin may benefit patients of dyslipidemia with type 2 diabetes (The ACCORD Study Group, 2010). Chronic hyperglycemia in diabetes invokes the onset of micro-vascular complications, such as recurrent foot ulcerations and risk for amputation (Paneni *et al*., 2013). FIELD (Fenofibrate Intervention and Event Lowering in Diabetes) study demonstrates that the use of fenofibrate, irrespective of the presence of dyslipidemia, for the treatment of patients with type 2 diabetes significantly reduces the risk for minor amputations without large-vessel disease, probably through non-lipid mechanisms (Rajamani *et al*., 2009). However, mechanisms about fenofibrate on improving micro-vascular complications in hyperglycemia remain unclear. To understand the role of fenofibrate on angiogenesis in chronic hyperglycemia, with streptozotocin (STZ)-induced diabetic mice we tested our hypothesis that fenofibrate could accelerate wound healing by improving impaired EPCs function *via* inhibiting eNOS uncoupling.

Methods

Animals. Male C57BL/6 mice (6~8w,18~20g) were purchased from the Sino-British SIPPR/BK Lab Animal Ltd (Shanghai, China), housed in controlled conditions (temperature: 21±2℃ and lighting: 8:00-20:00) and received a standard mouse chow and tap water adlibitum. All the animals used in this work received humane care in compliance with the institutional animal care guidelines and the Guide for Care and Use of Laboratory Animals published by the National Institutes of Health.

Experimental protocols. Mice received streptozotocin (STZ; Amresco, Solon, Ohio; 60 mg/kg/d × 5d, intraperitoneally, *i.p.*) dissolved in 0.1mM sodium citrate buffer (pH 4.5) (King, 2012). On day 20, whole blood was obtained from the mouse tail vein and random glucose levels were measured using the blood glucose monitoring system (Maochang, Taibei, China). Mice with a blood glucose value ≥ 250 mg/dL were defined as STZ-induced diabetic mice. Citrate buffer-treated mice were served as control. STZ-induced diabetic mice were randomly divided into 2 groups and were treated with vehicle (0.5% Carboxyl Methyl Cellulose, CMC) or fenofibrate (FF; Sigma-Aldrich, St. Louis, MO, 100 mg/kg/d×14d, intragastric administration, *i.g.*) respectively (Huang *et al*., 2008; Srivastava *et al*., 2006). The control received vehicle. On day 34, mice were used for wound closure experiment, or anesthetized to harvest bone marrow to isolate EPCs (Figure 1).

Measurement of wound closure and angiogenesis. Mice (two STZ-induced diabetic mice groups and the control) were anesthetized with ketamine (100 mg/kg, *i.p.*), and the dorsum was clipped free of hair and swabbed with betadine and 75% ethanol three times before wounding. A 6 mm circular wound was created with a biopsy punch. The wound closure rate was measured by tracing each wound area with a clear, bioclusive transparent dressing (Johnson & Johnson, Arlington, TX, USA.) every 2 days from day 34 to day 46 (Figure 1) (Tie, 2009). The tracings were digitized, and the areas were calculated with Image-Pro Plus software (Media Cybernetics, Silver Spring, MD).

Wounds were harvested from mice on day 3, 6 and 9 after creating. Samples were fixed with 4% paraformaldehyde for 24 h, then embedded in paraffin and sectioned at 4-μm intervals. After deparaffinization and rehydration, slides were placed in Tris-buffered saline (pH 7.5) for 5 min. Endogenous peroxidase was blocked by immersing the slides for 20 minutes in a 3% hydrogen peroxide/methanol bath, followed by distilled H_2O rinses. After treating with normal rabbit serum for 30 min (Vector Laboratories, Burlingame, CA), the slides were incubated for 60 min at room temperature with an anti-CD 31 antibody (1:50; BD Bioscience, San Jose, CA)，and further incubated with Vectastain Elite ABC Reagent (Vector Laboratories) for 30 min and Nova Red (Vector Laboratories) for 15 min. Slides were counterstained with Hematoxylin (VWR Scientific, Radnor, PA) for 10 sec, differentiated in 1% aqueous glacial acetic acid, and rinsed in running tap water. Two slides from each mouse were

examined; for each slide, five high-power fields (200×) were checked. Capillaries were recognized as tubular structures positive for CD31, and capillary density in the healing wounds was quantified. The number was summed and averaged as capillaries per high-power field.

Determination of EPCs function. Mouse bone marrow-derived EPCs were isolated, cultured and identified according to the method we previously established (Chen *et al*., 2013; also see Supplement). The ability of migration and tube formation was used to assess EPCs function. The migratory ability of EPCs was evaluated by a modified Boyden chamber assay. Briefly, 5×10^4 EPCs were placed in the upper chambers of 24-well Transwell plates per well (Corning Transwell, Lowell, MA) with polycarbonate membrane (8-μm pores) that contained serum-free endothelial growth medium; VEGF (50 ng/ml) was added to medium placed in the lower chambers. After incubation for 24h, the membrane was washed with PBS, fixed with 2% paraformaldehyde, and stained by Hoechst 33258 10μg/ml (Sigma-Aldrich, St. Louis, MO). The migrated cells were counted in 5 random low-power (×50) microscopic fields per sample.

The angiogenic capacity of EPCs was determined by Matrigel tube formation assay. Briefly, 4×10^4 EPCs were plated in 96-well plates per well precoated with 50μl/well growth factor-reduced Matrigel (BD Biosciences, Bedford, MA) and incubated at 37℃ for 6h. Tube formation ability of EPCs was assessed by counting tubes number with a computer-assisted microscope (Leica Microsystems Inc., Buffalo Grove, IL). Images of tube morphology were taken in 5 random low-power (×50) microscopic fields per sample.

Analysis of eNOS uncoupling in EPCs

Detection of Intracellular NO and Superoxide. Intracellular NO level was detected by membrane-permeable probes 4-amino-5-methylamine-2', 7'-difluorofluorescein (DAF-FM) diacetate (Invitrogen, Carlsbad, CA). EPCs were incubated with DAF-FM diacetate (10^{-6} mol/L) for 30 min at 37℃ and an additional 30 min at room temperature in dark. For determination of **i**ntracellular O_2^- level, dihydroethidium (DHE) (Invitrogen, Carlsbad, CA), a membrane-permeable dye oxidized to ethidium bromide in the presence of O_2^-, was used. EPCs were incubated with DHE (10^{-6}mol/L) for 30 min at 37℃ in dark. DAF and DHE images were obtained with a laser-scanning confocal microscope (Leica TCS SP2, Am Friedensplatz, Germany) at a magnification of × 60 using identical acquisition settings for each section. Fluorescence was quantified by automated image analysis with Image-Pro Plus software (Media Cybernetics, Silver Spring, MD). For each section, mean fluorescence was calculated from five separate low-power fields per view.

Determination of Tetrahydrobiopterin. Tetrahydrobiopterin **(**BH_4) in EPCs was determined by high-performance liquid chromatography (HPLC) with florescence detection after iodine oxidation in acidic or alkaline conditions (Fukushima and Nixon,

1980). The amount of BH_4 was determined from the difference between total (BH_4 plus BH_2 plus biopterin) and alkaline-stable oxidized (BH_2 plus biopterin) biopterin. A Nucleosil C-18 column (4.6 × 250 mm, 5 μm; Macher-Nagel, Duren, West Germany) was used with 5% methanol/95% water as a solvent at a flow rate of 1.0 ml/min. Fluorescence detection (350 nm excitation, 450 nm emission) was performed using a fluorescence detector (RF10AXL, Shimadzu Co., Kyoto, Japan). BH_4 concentrations, expressed as pmol/mg protein, were calculated by subtracting oxidized biopterin from total biopterins.

Western Blot Analysis for eNOS, phosphorylated eNOS, GTPCH1 and DHFR**.** EPCs were lysed, centrifuged at 12,000 g at 4°C for 15 min, and the supernatant was obtained. Protein was quantified by a BCA Protein Assay Kit (Thermo, Rockford, USA). Samples containing equal amounts of protein were run on 10% SDS-PAGE. The proteins were electrotransferred to nitrocellulose filter membranes. The membranes were incubated in PBS containing 5% non-fat dry milk for 4 h at 25°C. The blots were incubated overnight at 4°C with primary antibodies, and then incubated with secondary antibodies for 1 h at 25°C. Primary antibodies used included mouse anti-eNOS monoclonal antibody (1:1500; BD Transduction Laboratories, Lexington, Ky), rabbit polyclonal anti-phosphorylated eNOS (Ser-1177) antibody (1:1000; Cell Signaling Technology, Danvers, Mass), goat anti-GTPCH1 antibody (1:500; Abcam, Burlingame, CA), rabbit anti-DHFR antibody (1:1000; Abcam, Burlingame, CA), and mouse anti-actin (1:1000; Calbiochem, San Diego, CA). Secondary antibodies used included IRDye 800-conjugated anti-mouse antibody (1:3000; Rockland Immunochemical, Inc, Gilberts-ville, PA), and Alexa Fluor 680 goat anti-rabbit IgG antibody (1:3000; Invitrogen, Carlsbad, CA), Alexa Fluor 790 donkey anti-goat IgG antibody (1:3000; Abcam, Burlingame, CA). The images were visualized using Odyssey infrared imaging system (Li-Cor Bioscience, Lincoln, NE), and the bands were quantified by Image-Pro Plus software (Media Cybernetics, Silver Spring, MD).

Low-temperature SDS-PAGE eNOS dimer and monomer. EPCs extracts were mixed with 3 × SDS sample buffer (187.5 mmol/L Tris-HCl, pH 6.8; 6% wt/vol SDS; 30% glycerol; 0.03% wt/vol bromophenol blue; 15% vol/vol 2-mercaptoethanol) at 0°C. Samples were loaded on 7.5% polyacrylamide gels and subjected to electrophoresis. Both gels and buffers were cooled to 4°C before electrophoresis, and the buffer tank was placed in an ice bath during electrophoresis. eNOS dimer/monomer protein was measured by Western blot analysis.

***In Vitro* study.** EPCs was obtained from male C57BL/6 mice. After 7 days of culturing, medium were replaced with high glucose (33mM) medium or high glucose medium containing fenofibrate (5, 25 or 50 μM) for 24h (Marchetti *et al*., 2006), or fenofibrate (25μM) together with MK886 (a PPARα antagonist; 1μM). Effects of fenofibrate on high glucose induced EPCs dysfunction were assessed by functional analysis (migration and tube formation), and by measuring intracellular NO and O_2^-

levels.

Statistical analysis. Data were expressed as mean ± SEM. Experimental means were subjected to unpaired Student *t* test and 1-way ANOVA with Newman-Keuls multiple comparison test. A probability value of <0.05 was considered statistically significant.

Results

Streptozotocin-induced diabetic mice

Fifteen days after a 5-day low-dose STZ injection, blood glucose level in STZ-induced diabetic mice was significantly increased when compared with the control (367 ± 33 *vs* 127 ± 9 mg/dL, $P < 0.01$; Figure 2A), while the body weight was markedly decreased (19 ± 0.9 *vs* 25 ± 0.6 g, $P < 0.01$; Figure 2B). Two weeks treatment with fenofibrate did not modify the blood glucose level and body weight in STZ-induced diabetic mice (Figures 2C and 2D). The influence of fenofibrate on serum triglyceride (TG) and high-density lipoprotein cholesterol (HDL-C) in diabetic mice was shown in Figure S2.

Fenofibrate accelerated wound closure and angiogenesis in diabetic mice

To assess the effects of fenofibrate on wound closure in STZ-induced diabetic mice, the percentage of wound closure was measured every other day until day 12. As shown in figure 3, compared with the control, wound closure was significantly delayed in STZ-induced diabetic mice ($P < 0.05$, Figure 3). However, the percentage of wound closure in diabetic mice treated with fenofibrate was greater than that in the untreated diabetic mice ($P < 0.05$, Figure 3).

Capillary densities in the wounds and surrounding skin were calculated to evaluate the role of fenofibrate on capillary formation in diabetic mice. Compared with the control, capillary formation in STZ-induced diabetic mice was significantly worse on day 3, 6 and 9 ($P < 0.01$, Figure 4). Fenofibrate treatment significantly increased the capillary densities in diabetic mice on day 6 and 9 when compared with the untreated diabetic ones ($P < 0.01$, Figure 4), though fenofibrate did not augment capillary formation on day 3. These data demonstrate that fenofibrate is effective to enhance angiogenesis in diabetic wound healing.

Fenofibrate improved EPCs function of diabetic mice

To understand whether the accelerated wound healing in diabetic mice were potentially mediated by the improvement of EPCs function, the capacities of migration and tube formation of EPCs were assessed. It was found that EPCs from STZ-induced diabetic mice showed significantly decreased cell migration and tube formation capacities as compared with the control group. Fenofibrate treatment significantly increased both the capacities of migration (1.01 ± 0.05 *vs* 0.45 ± 0.03, $P < 0.01$) and tube formation (0.83 ± 0.09 *vs* 0.49 ± 0.05, $P < 0.01$) in STZ-induced diabetic mice when compared with the untreated diabetic ones (Figure 5A-5D).

Similarly, the percentage of circulating EPCs in STZ-induced diabetic mice was markedly reduced as compared with the control (1.31 ± 0.03 *vs* 3.32 ± 0.02, $P < 0.01$), and fenofibrate treatment prevented this reduction in diabetic mice (Figure 5E and 5F). However, fenofibrate treatment for the control (normal mice) did not modify EPCs function, and circulating EPCs number (Figure S3A-S3F).

Fenofibrate increased eNOS phosphorylated-to-total and dimer-to-monomer ratio in EPCs of diabetic mice

Western blot analysis found that total eNOS protein expression in EPCs showed no difference among groups (Control: 1.00 ± 0.11, STZ: 1.16 ± 0.12, STZ+FF: 0.99 ± 0.11). However, both the eNOS phosphorylated-to-total and dimer-to-monomer ratio in EPCs were significantly decreased in STZ-induced diabetic mice when compared with the control. Fenofibrate treatment significantly reversed the decreased eNOS phosphorylated-to-total (0.87 ± 0.05 *vs* 0.48 ± 0.03, $P < 0.01$) and dimer-to-monomer (0.93 ± 0.04 *vs* 0.67 ± 0.02, $P < 0.01$) ratio in EPCs of diabetic mice (Figure 6).

Fenofibrate restored BH_4 levels and increased GTPCH1 in EPCs of diabetic mice

Reduced BH_4 levels have been reported to be involved in diabetic eNOS uncoupling. Thus, intracellular levels of total and oxidized biopterin, and BH_4 levels were measured in EPCs. It was found that total biopterin in EPCs had no significant differences among three groups (Control: 32 ± 1.8, STZ: 31 ± 2.1, STZ+FF: 34 ± 0.5 pmol/mg; Figure 7A). STZ-induced diabetic mice exhibited greater level of oxidized biopterin when compared the control (24 ± 1.2 *vs* 18 ± 1.4 pmol/mg, $P < 0.05$), and fenofibrate treatment completely prevented this increase (Figure 7B). BH_4 level was significantly lower in STZ-induced diabetic mice as compared with the control (9 ± 0.6 *vs* 13 ± 1.2 pmol/mg, $P < 0.05$), and fenofibrate treatment restored the BH_4 level in EPCs in diabetic mice to a level similar to that in the control (Figure 7C). In addition, treatment with exogenous BH_4 improved the tube formation capacity of EPCs from diabetic mice similar to that of fenofibrate (Figure S5).

The BH_4 levels are regulated by de novo (GTPCH1) or salvage (DHFR) pathway. We next investigated the mechanism of restoration of BH_4 by fenofibrate. It was found that GTPCH1 expression was decreased in EPCs from diabetic mice when compared with the control, which was reversed by fenofibrate treatment (0.77 ± 0.04 vs 0.41 ± 0.03, $P < 0.01$). However, the DHFR level displayed no changes among three groups (Figure 7D-7F).

Fenofibrate attenuated eNOS uncoupling in EPCs of diabetic mice

To test whether restoration of BH_4 in EPCs in diabetic mice attenuated eNOS uncoupling and enhanced its regular enzymatic activity, and subsequently increased NO production and inhibited O_2^- formation, intracellular NO and O_2^- levels were measured. The NO level in EPCs was significantly reduced in STZ-induced diabetic mice when compared with the control, fenofibrate treatment for diabetic mice increased the NO level (0.72 ± 0.04 *vs* 0.43 ± 0.06, $P < 0.01$ Figure 8A and 8B). On

the contrary, the O_2^- level in EPCs from STZ-induced diabetic mice was significantly elevated, fenofibrate treatment for diabetic mice prevented this elevation (1.48 ± 0.09 *vs* 2.10 ± 0.18, $P < 0.01$; Figure 8C and 8D). However, fenofibrate treatment for the control (normal mice) did not modify both intracellular NO and O_2^- levels (Figure S3G-S3J). In addition, after NOS inhibition with (Nω-Nitro-L-arginine) L-NNA in EPCs from diabetic mice, O_2^- production was significantly reduced when compared with the ones without L-NNA treatment (1.36 ± 0.14 *vs* 1.86 ± 0.08, $P < 0.01$; Figure 8E and 8F). These demonstrated that eNOS in EPCs of diabetic mice contributes to O_2^- formation.

Fenofibrate attenuated high glucose-induced EPCs dysfunction and eNOS uncoupling

To investigate whether results from the animal study could be related to the increased glucose concentration in mice, high glucose was used to induce EPCs dysfunction. High glucose treatment impaired both the capacity of migration and tube formation of cultured EPCs. Fenofibrate (5, 25 and 50 μM) treatment improved impaired EPCs function caused by high glucose (Figures 9A, 9B, 9E and 9F). High glucose also resulted in decreased NO production and increased O_2^- formation as compared with the control. Similarly, fenofibrate (5, 25 and 50 μM) treatment reversed these changes (Figure 9C, 9D, 9G and 9H). In addition, MK886 (a PPARα antagonist) failed to block the effect of fenofibrate on cell migration and tube formation, and intracellular O_2^- and NO production (Figure S6), suggesting that these effects of fenofibrate on EPCs might be PPARα independent.

Discussion & conclusions

The main findings of this study are: fenofibrate treatment could accelerate wound healing, recover the impaired EPCs capacities, prevent eNOS uncoupling, and increase BH_4 levels in EPCs of STZ-induced diabetic mice. *In vitro*, fenofibrate dose dependently reversed high glucose-impaired EPCs functions, and enhanced NO level while inhibited O_2^- production. Thus, we for the first time demonstrated that fenofibrate could improve high glucose-impaired EPCs functions by inhibiting eNOS uncoupling though a BH_4-related mechanism in STZ-induced diabetic mice.

Wound healing is an integrative and well-coordinated regenerative response to tissue injury (Jeffcoate and Harding, 2003). Under diabetic condition, vascular repair is reduced and wound healing is significantly delayed (Dinh *et al*., 2012; Liu *et al*., 2014). In addition, chronic hyperglycemia in diabetes is believed to be responsible for the onset of microvascular complications, including the recurrence of foot ulcerations and risk for amputation (Kulkarni *et al*., 2014; Pradhan *et al*., 2009). Fenofibrate, a PPARα agonist, mainly used in the treatment of dyslipidemia in the clinic, was demonstrated to be effective in reducing the risk for minor amputations probably through non-lipid mechanisms in patients with type 2 diabetes (Rajamani *et al*., 2009; Ting *et al*., 2012). The FIELD study also indicated that fenofibrate treatment significantly reduced the risk of total cardiovascular disease events, particularly

through the prevention of non-fatal myocardial infarctions and coronary revascularizations, and could also significantly reduce microvascular-associated complications in type 2 diabetic patients (Keech *et al*., 2005). In this work, STZ-induced diabetic mice received fenofibrate 100 mg/kg/d intragastrically for a successive 14 d. Though this treatment did not change both the blood glucose level and the body weight, it did increase the capillary densities and the percentage of wound closure in STZ-induced diabetic mice. We therefore explored the mechanism of fenofibrate in accelerating wound healing in diabetes.

Endothelial monolayer is essential for maintaining the quiescence and integrity of vasculature (Dejana *et al*., 2009). Under some pathological conditions, such as in diabetic patients, the functional activity and even the structure of endothelial cells are damaged, which may contribute to micro- and macro- vascular abnormalities (Paneni *et al*., 2013; Lee *et al*., 2013). EPCs, a group of multi-progenitor cells, having the ability to differentiate into endothelial cells and contributing to endothelial recovery (Asahara *et al*., 1997; Lee and Yoon, 2013) plays a critical role in vascular endothelium integrity, in vascular repair and regeneration (Inoue *et al*., 2011; Liu *et al*., 2011). Accumulating evidences demonstrated that with the occurrence of EPCs dysfunction, the number of circulating EPCs was significantly decreased in diabetes and atherosclerosis (Werner *et al*., 2014; Westerweel *et al*., 2013). Studies have shown that EPCs, as important precursors of endothelial cells, is involved in angiogenesis and wound repair (Pradan *et al*., 2009). Importantly, systematic administration of EPCs could significantly improve angiogenesis and wound healing in diabetic mice (Marrotte *et al*., 2010). These suggest that it might be clinically significance to increase circulating EPCs number and/or to improve EPCs functions with certain specific drugs in the treatment for diabetes, especially for diabetic vascular complications. Compared with the control, we found that circulating EPCs was significantly increased, and the migration and tube formation capacities of EPCs was markedly augmented after 14 days fenofibrate administration in STZ-induced diabetic mice. Thus, we postulated that the effect of fenofibrate in accelerating wound healing under diabetic condition was possibly related to recover impaired EPCs function and to increase circulating EPCs number.

Dysfunction of EPCs contributes to the pathogenesis of diabetes, and the main cause of EPCs dysfunction is the loss of protection from NO due to reduced synthesis from eNOS (Thum *et al*., 2007). In EPCs, eNOS is the uniquely expressed NOS isoform, and both iNOS and neuronal NOS are not detected (Förstermann and Sessa, 2012). Generally, increased eNOS expression is considered to be beneficial. However, under certain pathophysiological conditions, eNOS expression is not positively related to endothelium-dependent vasodilatation (Alp *et al*., 2003) explained by the so-called "eNOS uncoupling" (Förstermann and Munzel, 2006) which was shown in a variety of experimental and clinical vascular disease states, especially in diabetes (Guzik *et al*., 2002; Alp and Channon, 2004). In diabetic EPCs, though total eNOS expression might be unchanged or even increased, phosphorylated eNOS level was significantly decreased. In addition, eNOS dimer-to-monomer ratio was significantly reduced (Thum *et al*., 2007). In this work, we found that total eNOS protein displayed no

changes among three groups (Control, STZ, and STZ+FF), and fenofibrate treatment increased eNOS phosphorylated-to-total and dimer-to-monomer ratio in EPCs of STZ-induced diabetic mice to levels similar to those in the controls. We also found that mRNA level of eNOS in EPCs was significantly decreased in STZ-induced diabetic mice when compared with the control, and fenofibrate treatment dramatically increased its expression (Figure S4). These indicated that it was the phosphorylated eNOS protein, but not the total eNOS protein, was consistent with the mRNA level of eNOS. This was a little difficult to understand, but it conformed to the results reported by Poittevin *et al*. (Poittevin *et al*., 2014). It was demonstrated that the dimeric form of eNOS appeared to be biochemically active and was able to generate either NO or O_2^-, whereas the monomeric form of eNOS could be viewed as a marker for eNOS uncoupling (Bauersachs and Schafer, 2005). The result that fenofibrate treatment recovered the eNOS dimer-to-monomer ratio suggested that fenofibrate could prevent eNOS uncoupling in diabetic EPCs.

Under the condition of eNOS uncoupling, eNOS itself can produce O_2^- instead of NO (Gielis *et al*., 2011). In the present study, we found that NO level was decreased and O_2^- production was increased in EPCs of diabetic mice. *In vitro*, EPCs dysfunction was accompanied by decreased NO level and increased O_2^- production caused by high glucose. However, fenofibrate treatment prevented these changes. Finally, the fact that NOS inhibition by L-NNA decreased O_2^- production in EPCs from diabetic mice indicated that eNOS uncoupling in EPCs was existed in STZ-induced diabetic mice and was involved in exaggerated O_2^- production. These together confirmed that eNOS uncoupling was developed in EPCs under high glucose environments, and further suggested that fenofibrate could prevent eNOS uncoupling in diabetic EPCs.

The underlying mechanism by which eNOS uncoupling occurs is still unclear. Evidence indicates the level of the eNOS essential cofactor, BH_4, is an important determinant for eNOS uncoupling. When BH_4 levels are decreased, NO production is then switched to O_2^- production, further reducing the activity of such NO as is produced, thus contributing to vascular oxidative stress and EPCs dysfunction (Du *et al*., 2008). In cells, total biopterin includes BH_4, BH_2 and biopterin (BH_2 and biopterin are the oxidized forms of biopterin). The levels of intracellular BH_4 depend by large on their degradation due to excessive oxidation (The ACCORD Study Group, 2010). In diabetes, it has been demonstrated that reduced BH_4 levels contributes to eNOS uncoupling (Abudukadier *et al*., 2013), and restoration of BH_4 can "recouple" eNOS and enhance its regular enzymatic activity leading to produce NO rather than O_2^- (Moens *et al*., 2008; Teng *et al*., 2011). In the present study, we found that total biopterin was not changed, and oxidized biopterin was significantly increased, while BH_4 displayed a significant decrease in EPCs from STZ-induced diabetic mice. Fenofibrate treatment increased the BH_4 levels in EPCs from diabetic mice similar to that in the control. With the restoration of BH_4 levels, NO production was increased and O_2^- production was decreased in diabetic EPCs. These strongly supported that fenofibrate could prevent BH_4 degradation and increase BH_4 levels in diabetic EPCs.

BH_4 levels are determined by the activity of GTPCH1, the rate-limiting enzyme in

de novo BH_4 biosynthesis, as well as the activity of DHFR which can regenerate BH_4 from BH_2 (Crabtree *et al.,* 2009). It was reported that GTPCH1 was down-regulated and the DHFR was up-regulated in diabetic rats (Wenzel *et al.,* 2008). In our work, we found that fenofibrate significantly increased the GTPCH1 expression but did not modify DHFR expression. These suggested that fenofibrate regulated BH_4 levels by the *de novo* pathway.

Recently Watson hypothesized that reactive oxygen species (ROS), such as O_2^-, might be necessary to stabilize about one third of proteins for generating their 3D shapes. Diabetes, cardiovascular diseases and some cancers might be accelerated by failure of generating sufficient ROS. These suggest it may be indispensable to keep a certain level of intracellular ROS as a treatment for diabetes (Watson, 2014). Interestingly, in this study we found that fenofibrate (100 mg/kg/d×14d, *i.g.*) decreased the O_2^- production and increased the NO level in EPCs of diabetic mice similar to those in controls. *In vitro*, fenofibrate (5-25 μM) could rectify the changed O_2^- and NO production caused by high glucose. Thus, we postulate that fenofibrate is able to keep a balance between the levels of ROS and NO production to benefit diabetes.

We conclude that fenofibrate could accelerate wound healing in STZ-induced diabetic mice by improving the impaired EPCs function *via* preventing eNOS uncoupling possibly related to increase intracellular BH_4 levels in EPCs. These suggest that fenofibrate, mainly used in the treatment of dyslipidemia, deserves repurposing for the treatment of diabetes, especially for reducing the risk of amputations in diabetes.

Acknowledgement:

This study was supported by the grants from National Natural Science Foundation of China (81370558, 81300081), from Natural Science Foundation of Zhejiang (20131813A20, 20130733Q41), and from Tongji University (2013KJ068).

Conflict of Interest: None.

References

Abudukadier A, Fujita Y, Obara A, Ohashi A, Fukushima T, Sato Y *et al*. (2013). Tetrahydrobiopterin has a glucose-lowering effect by suppressing hepatic gluconeogenesis in an endothelial nitric oxide synthase-dependent manner in diabetic mice. Diabetes 62: 3033-3043.

Alp NJ, Mussa S, Khoo J, Cai S, Guzik T, Jefferson A *et al*. (2003). Tetrahydrobiopterin-dependent preservation of nitric oxide-mediated endothelial

function in diabetes by targeted transgenic GTP-cyclohydrolase I overexpression. J Clin Invest 112: 725-735.

Alp NJ, Channon KM (2004). Regulation of endothelial nitric oxide synthase by tetrahydrobiopterin in vascular disease. Arterioscler Thromb Vasc Biol 24: 413-420.

Asahara T, Murohara T, Sullivan A, Silver M, van der Zee R, Li T *et al*. (1997). Isolation of putative progenitor endothelial cells for angiogenesis. Science 275: 964-967.

Bauersachs J, Schafer A (2005). Tetrahydrobiopterin and eNOS dimer/monomer ratio--a clue to eNOS uncoupling in diabetes. Cardiovasc Res 65: 768-769.

Briguori C, Testa U, Riccioni R, Colombo A, Petrucci E, Condorelli G *et al*. (2010). Correlations between progression of coronary artery disease and circulating endothelial progenitor cells. FASEB J 24: 1981-1988.

Cassuto J, Dou H, Czikora I, Szabo A, Patel VS, Kamath V, et al. (2014). Peroxynitrite disrupts endothelial caveolae leading to eNOS uncoupling and diminished flow-mediated dilation in coronary arterioles of diabetic patients. Diabetes 63: 1381-1393.

Chen JK, Deng YP, Jiang GJ, Liu YZ, Zhao T, Shen FM (2013). Establishment of tube formation assay of bone marrow-derived endothelial progenitor cells. CNS Neurosci Ther 19: 533-535.

Crabtree MJ, Tatham AL, Hale AB, Alp NJ, Channon KM (2009). Critical role for tetrahydrobiopterin recycling by dihydrofolate reductase in regulation of endothelial nitric-oxide synthase coupling: relative importance of the de novo biopterin synthesis versus salvage pathways. J Biol Chem 284: 28128-28136.

Dejana E, Tournier-Lasserve E, Weinstein BM (2009). The control of vascular integrity by endothelial cell junctions: molecular basis and pathological implications. Dev Cell 16: 209-221.

Dinh T, Tecilazich F, Kafanas A, Doupis J, Gnardellis C, Leal E *et al*. (2012). Mechanisms involved in the development and healing of diabetic foot ulceration. Diabetes 61: 2937-2947.

Du YH, Guan YY, Alp NJ, Channon KM, Chen AF (2008). Endothelium-specific GTP cyclohydrolase I overexpression attenuates blood pressure progression in salt-sensitive low-renin hypertension. Circulation 117: 1045-1054.

Fleissner F, Thum T (2011). Critical role of the nitric oxide/reactive oxygen species

balance in endothelial progenitor dysfunction. Antioxid Redox Signal 15: 933-948.

Förstermann U, Munzel T (2006). Endothelial nitric oxide synthase in vascular disease: from marvel to menace. Circulation 113: 1708-1714.

Förstermann U, Li H (2011). Therapeutic effect of enhancing endothelial nitric oxide synthase (eNOS) expression and preventing eNOS uncoupling. Br J Pharmacol 164(2): 213-223.

Förstermann U, Sessa WC (2012). Nitric oxide synthases: regulation and function. Eur Heart J 33: 829-837.

Fukushima T, Nixon JC (1980). Analysis of reduced forms of biopterin in biological tissues and fluids. Anal Biochem 102: 176-188.

Gielis JF, Lin JY, Wingler K, Van Schil PE, Schmidt HH, Moens AL (2011). Pathogenetic role of eNOS uncoupling in cardiopulmonary disorders. Free Radic Biol Med 50: 765-776.

Guzik TJ, Mussa S, Gastaldi D, Sadowski J, Ratnatunga C, Pillai R *et al*. (2002). Mechanisms of increased vascular superoxide production in human diabetes mellitus: role of NAD(P)H oxidase and endothelial nitric oxide synthase. Circulation 105: 1656-1662.

Hamed S, Brenner B, Roguin A (2011). Nitric oxide: a key factor behind the dysfunctionality of endothelial progenitor cells in diabetes mellitus type-2. Cardiovasc Res 91: 9-15.

Huang Z, Zhou X, Nicholson AC, Gotto AM Jr, Haijar DP, Han J (2008). Activation of peroxisome proliferator-activated receptor-alpha in mice induces expression of the hepatic low-density lipoprotein receptor. Br J Pharmacol 155: 596-605.

Inoue T, Croce K, Morooka T, Sakuma M, Node K, Simon DI (2011). Vascular inflammation and repair: implications for re-endothelialization, restenosis, and stent thrombosis. JACC Cardiovasc Interv 4: 1057-1066.

Jeffcoate WJ, Harding KG (2003). Diabetic foot ulcers. Lancet 361: 1545-1551.

Kar P, Holt RI (2008). The effect of sulphonylureas on the microvascular and macrovascular complications of diabetes. Cardiovasc Drugs Ther 22: 207-213.

Keech A, Simes RJ, Barter P, Best J, Scott R, Taskinen MR, *et al.* (2005). Effects of long-term fenofibrate therapy on cardiovascular events in 9795 people with type 2 diabetes mellitus (the FIELD study): randomised controlled trial. Lancet 366:

1849-1861.

Kim JA, Montagnani M, Koh KK, Quon MJ (2006). Reciprocal relationships between insulin resistance and endothelial dysfunction: molecular and pathophysiological mechanisms. Circulation 113: 1888-1904.

King AJ (2012). The use of animal models in diabetes research. Br J Pharmaco 166: 877-894.

Kulkarni M, O'Loughlin A, Vazquez R, Mashayekhi K, Rooney P, Greiser U *et al.* (2014). Use of a fibrin-based system for enhancing angiogenesis and modulating inflammation in the treatment of hyperglycemic wounds. Biomaterials 35: 2001-2010.

Lee S, Yoon YS (2013). Revisiting cardiovascular regeneration with bone marrow-derived angiogenic and vasculogenic cells. Br J Pharmacol 169: 290-303.

Liu F, Chen DD, Sun X, Xie HH, Yuan H, Jia WP *et al*. (2014). Hydrogen Sulfide Improves Wound Healing via Restoration of Endothelial Progenitor Cell Functions and Activation of Angiopoietin-1 in Type 2 Diabetes. Diabetes 63: 1763-1778.

Liu L, Wei H, Chen F, Wang J, Dong JF, Zhang J (2011). Endothelial progenitor cells correlate with clinical outcome of traumatic brain injury. Crit Care Med 39: 1760-1765.

Marchetti V, Menghini R, Rizza S, Vivanti A, Feccia T, Lauro D *et al*. (2006). Benfotiamine counteracts glucose toxicity effects on endothelial progenitor cell differentiation via Akt/FoxO signaling. Diabetes 55: 2231-2237.

Marrotte EJ, Chen DD, Hakim JS, Chen AF (2010). Manganese superoxide dismutase expression in endothelial progenitor cells accelerates wound healing in diabetic mice. J Clin Invest 120: 4207-4219.

Moens AL, Takimoto E, Tocchetti CG, Chakir K, Bedja D, Cormaci G *et al*. (2008). Reversal of cardiac hypertrophy and fibrosis from pressure overload by tetrahydrobiopterin: efficacy of recoupling nitric oxide synthase as a therapeutic strategy. Circulation 117: 2626-2636.

Paneni F, Beckman JA, Creager MA, Cosentino F (2013). Diabetes and vascular disease: pathophysiology, clinical consequences, and medical therapy: part I. Eur Heart J 34: 2436-2443.

Poittevin M, Bonnin P, Pimpie C, Rivière L, Sebrié C, Dohan A, *et al*. (2014). Diabetic microangiopathy: impact of impaired cerebral vasoreactivity and delayed angiogenesis after permanent middle cerebral artery occlusion on stroke damage and

cerebral repair in mice. Diabetes Epub ahead of print.

Pradhan L, Nabzdyk C, Andersen ND, LoGerfo FW, Veves A (2009). Inflammation and neuropeptides: the connection in diabetic wound healing. Expert Rev Mol Med 11: e2.

Rajamani K, Colman PG, Li LP, Best JD, Voysey M, D'Emden MC *et al*. (2009). Effect of fenofibrate on amputation events in people with type 2 diabetes mellitus (FIELD study): a prespecified analysis of a randomised controlled trial. Lancet 373: 1780-1788.

Srivastava RA, Jahagirdar R, Azhar S, Sharma S, Bisgaier CL (2006). Peroxisome proliferator-activated receptor-alpha selective ligand reduces adiposity, improves insulin sensitivity and inhibits atherosclerosis in LDL receptor-deficient mice. Mol Cell Biochem 285: 35-50.

Teng RJ, Du J, Xu H, Bakhutashvili I, Eis A, Shi Y *et al*. (2011). Sepiapterin improves angiogenesis of pulmonary artery endothelial cells with in utero pulmonary hypertension by recoupling endothelial nitric oxide synthase. Am J Physiol Lung Cell Mol Physiol 301: L334-345.

The ACCORD Study Group (2010). Effects of combination lipid therapy in type 2 diabetes mellitus. N Engl J Med 362: 1563-1574.

Thum T, Fraccarollo D, Schultheiss M, Froese S, Galuppo P, Widder JD *et al*. (2007). Endothelial nitric oxide synthase uncoupling impairs endothelial progenitor cell mobilization and function in diabetes. Diabetes 56: 666-674.

Tie L, Li XJ, Wang X, Channon KM, Chen AF (2009). Endothelium-specific GTP cyclohydrolase I overexpression accelerates refractory wound healing by suppressing oxidative stress in diabetes. Am J Physiol Endocrinol Metab 296:E1423-E1429.

Ting RD, Keech AC, Drury PL, Donoghoe MW, Hedley J, Jenkins AJ *et al*. (2012). Benefits and safety of long-term fenofibrate therapy in people with type 2 diabetes and renal impairment: the FIELD Study. Diabetes Care 35: 218-225.

Tousoulis D, Papageorgiou N, Androulakis E, Siasos G, Latsios G, Tentolouris K *et al*. (2013). Diabetes mellitus-associated vascular impairment: novel circulating biomarkers and therapeutic approaches. J Am Coll Cardiol 62: 667-676.

Wang Q, Zhang M, Ding Y, Wang Q, Zhang W, Song P *et al*. (2014). Activation of NAD(P)H oxidase by tryptophan-derived 3-hydroxykynurenine accelerates endothelial apoptosis and dysfunction in vivo. Circ Res 114: 480-492.

Watson JD (2014). Type 2 diabetes as a redox disease. Lancet 383: 841-843.

Wenzel P, Daiber A, Oelze M, Brandt M, Closs E, Xu J, *et al*. (2008) Mechanisms underlying recoupling of Enos by HMG-CoA reductase inhibition in a rat model of streptozotocin-induced diabetes mellitus. Atherosclerosis 198: 65-76.

Werner CM, Schirmer SH, Gensch C, Pavlickova V, Pöss J, Wright MB *et al*. (2014). The dual PPARα/γ agonist aleglitazar increase the number and function of endothelial progenitor cells: implications for vascular function and atherogenesis. Br J Pharmacol 171: 2685-2703.

Westerweel PE, Teraa M, Rafii S, Jaspers JE, White IA, Hooper AT *et al*. (2013). Impaired endothelial progenitor cell mobilization and dysfunctional bone marrow stroma in diabetes mellitus. PLoS One 8: e60357.

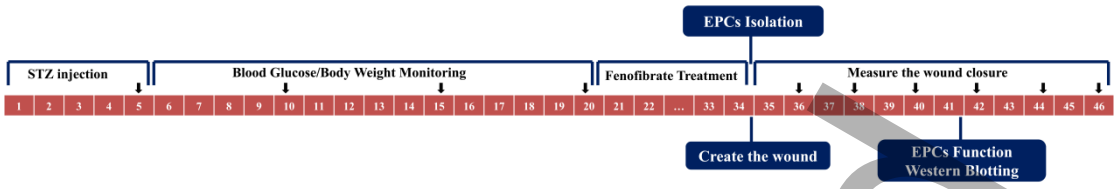

Figure 1

Figure 1. Illustration of experimental schedule. Mice were subjected to streptozotocin (STZ) for 5 consecutive days, and blood glucose was monitored every 5 days until day 20, and then received fenofibrate treatment for 14 days, finally the mice were used for wound closure experiment or for EPCs isolation.

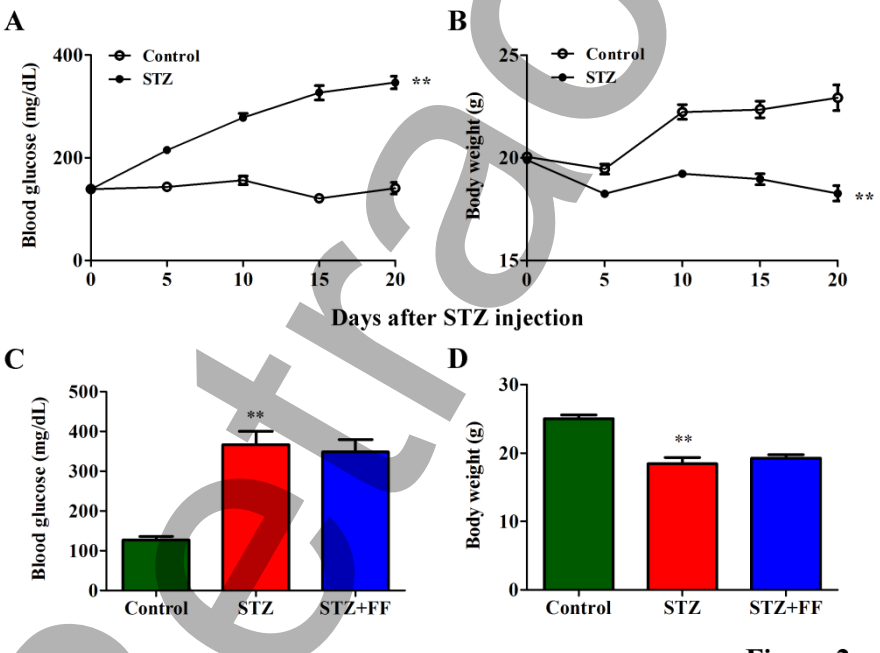

Figure 2

Figure 2. Changes of blood glucose concentration and body weight of streptozotocin-induced diabetic mice (STZ). Blood glucose (A) and body weight (B) changes of STZ (60 mg/kg×5d, *i.p.*) treated mice, which was defined as diabetic mice (blood glucose value ≥ 250 mg/dL)15 days after STZ treatment. Blood glucose (C) and body weight (D) changes of STZ-induced diabetic mice after fenofibrtate administration (FF, 100 mg/kg/d×14d, *i.g.*). Values are mean ± SEM. n=10 per group. $^{**}P < 0.01$ *vs* Control.

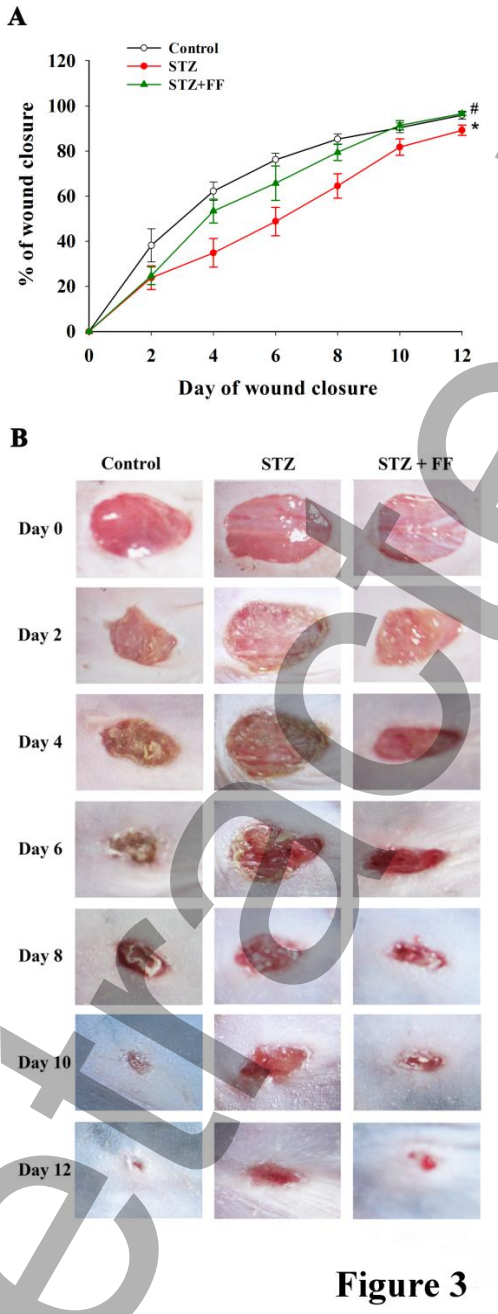

Figure 3

Figure 3. Fenofibrate (FF) accelerated wound healing in streptozotocin-induced diabetic mice (STZ). Six-mm diameter wound was made by punch biopsy and wound closure was measured every 2 days until day 12. (A) Fenofibrate accelerated the percentage of wound closure in STZ-induced diabetic mice as compared with the untreated diabetic ones. (B) Representative photographs of wound healing. Values are mean ± SEM. n=8 per group. $^{*}P < 0.05$ *vs* Control; $^{\#}P < 0.05$ *vs* STZ.

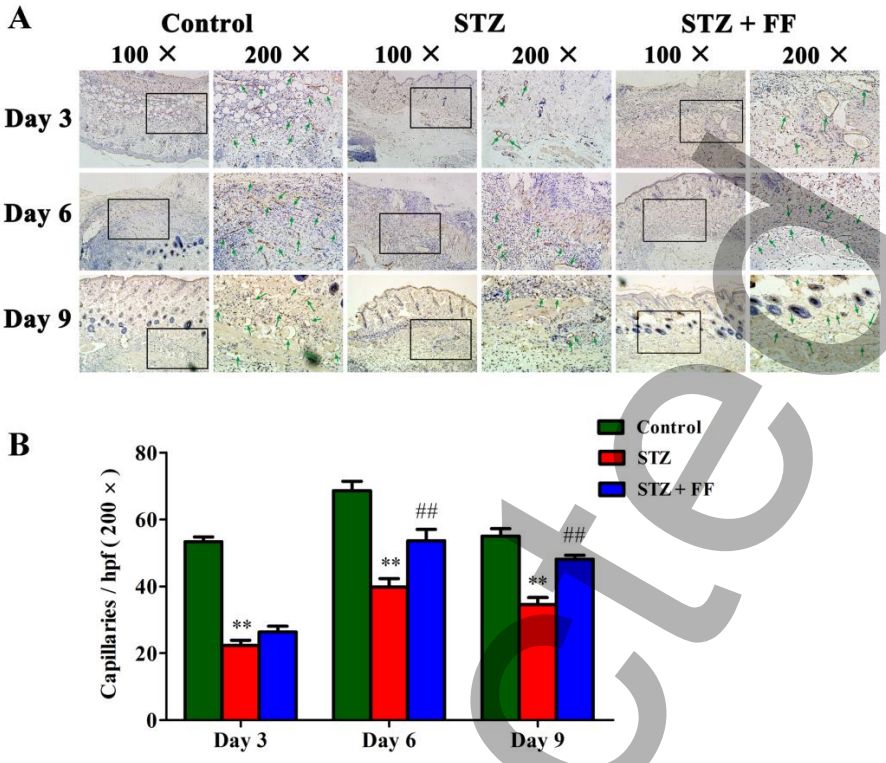

Figure 4

Figure 4. Fenofibrate (FF) enhanced wound angiogenesis in streptozotocin -induced diabetic mice (STZ). Six-mm diameter wound was made by punch biopsy and wound angiogenesis was measured on day 3, 6 and 9. (A) Representative photomicrographs of CD31 staining; green arrows point to CD31-positive capillaries; boxed regions (100×) are shown at higher magnification (200×) to the right. (B) Quantitative analysis of capillaries per high-power field (hpf) showed that wound capillaries in FF treated diabetic mice were increased on day 6 and 9 when compared with the untreated diabetic ones. Values are mean ± SEM. n=12 per group. $^{**}P < 0.01$ *vs* Control; $^{\#\#}P < 0.01$ *vs* STZ.

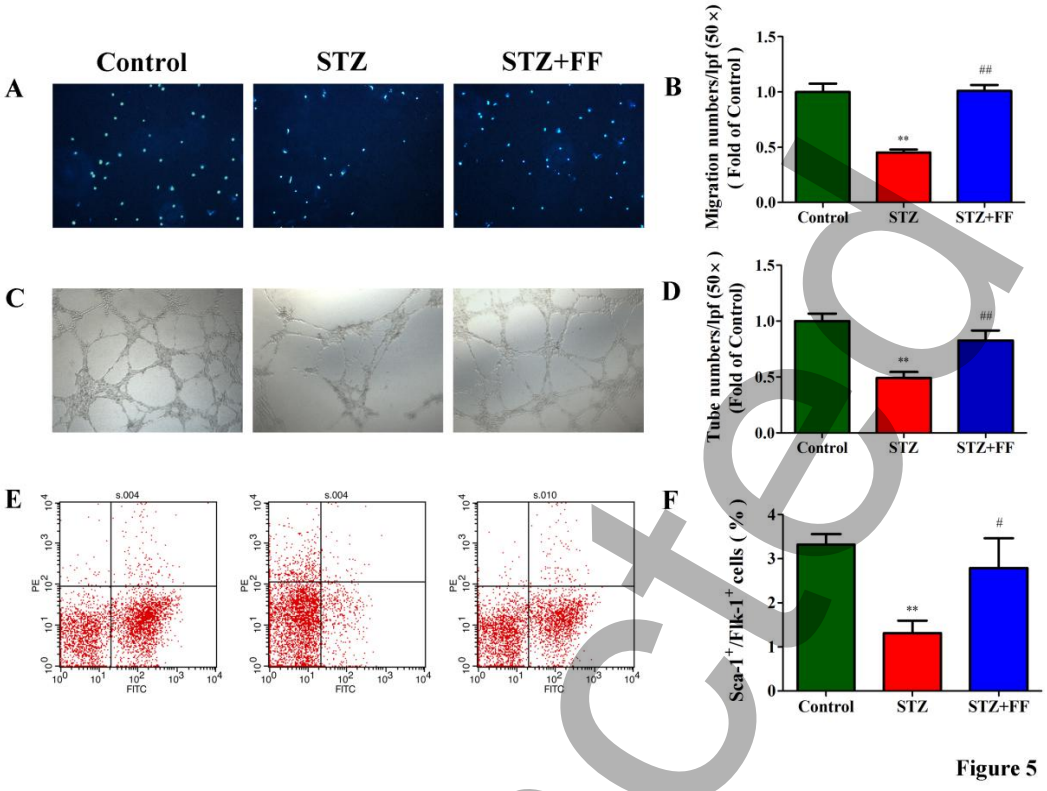

Figure 5

Figure 5. Fenofibrate (FF) improved EPCs functions of streptozotocin-induced diabetic mice (STZ). (A and B) Fenofibrate enhanced the migratory capacity of EPCs of diabetic mice. (C and D) Fenofibrate enhanced the tube formation capacity of EPCs of diabetic mice. (E and F) Fenofibrate increased the circulating EPCs number of diabetic mice. Values are mean ± SEM. n=5-8 per group. $^{**}P < 0.01$ *vs* Control; $^{\#}P < 0.05$, $^{\#\#}P < 0.01$ *vs* STZ.

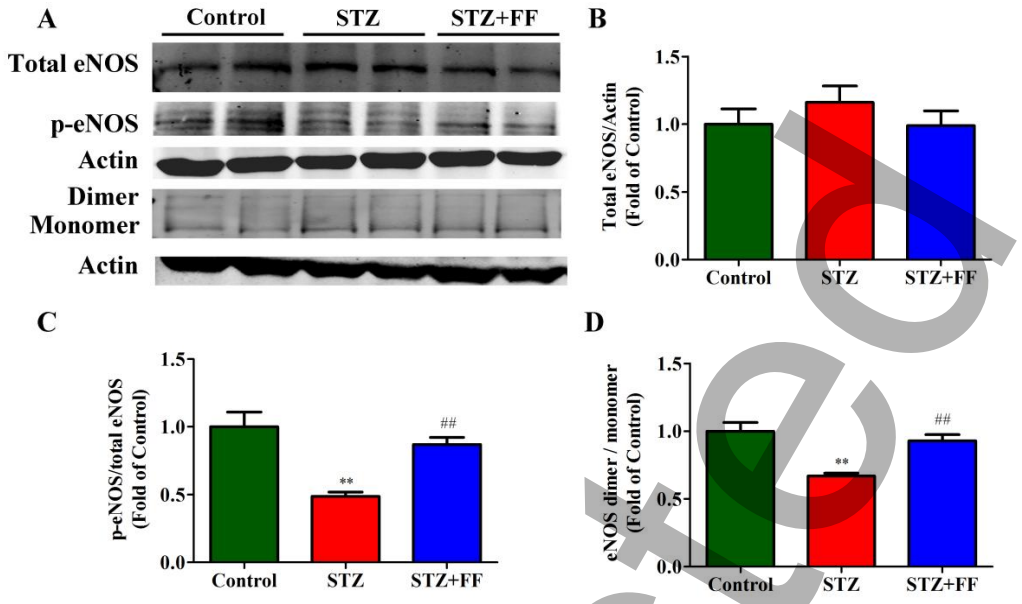

Figure 6

Figure 6. Fenofibrate (FF) led to increased eNOS phosphorylated-to-total and dimer-to-monomer ratio in EPCs of STZ-induced diabetic mice (STZ). (A) Western blot analysis was used to determine changes of eNOS expression in EPCs of STZ-induced diabetic mice with or without fenofibrate treatment. (B) Total eNOS expression. (C) Ratio of eNOS phosphorylated-to-total expression. (D) Ratio of eNOS dimer-to-monomer expression. Values are mean ± SEM. n=5 per group. $^{**}P<0.01$ *vs* Control; $^{\#\#}P < 0.01$ *vs* STZ.

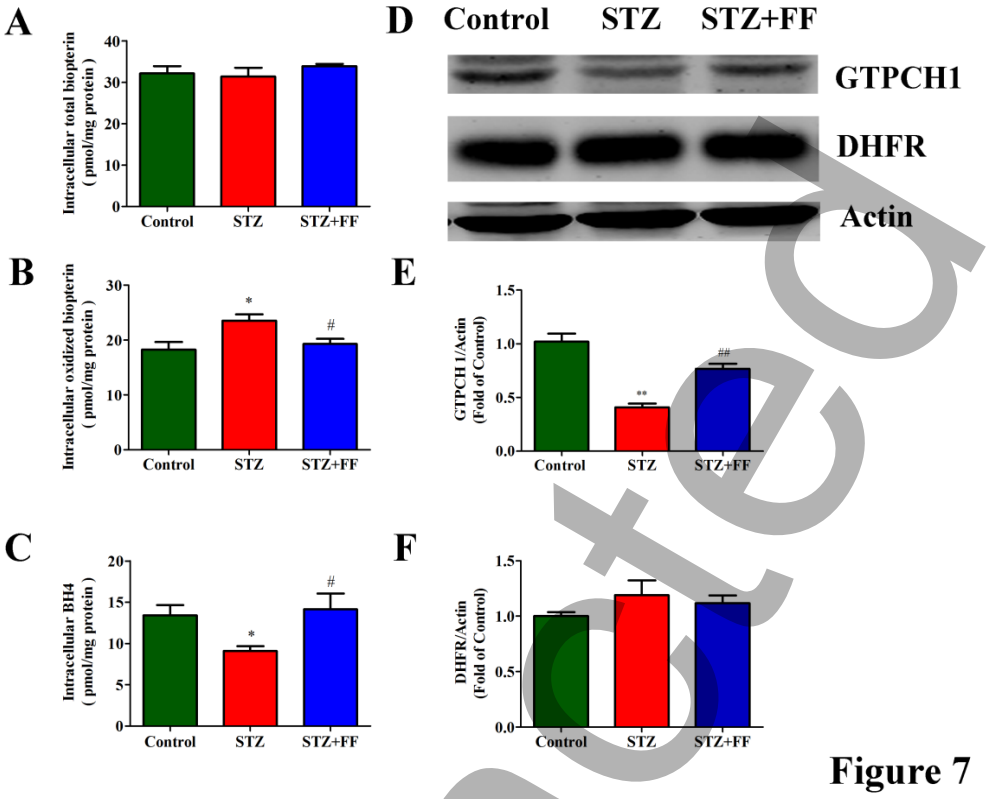

Figure 7. Fenofibrate (FF) restored intracellular BH_4 levels and increased the expression of GTPCH1 in EPCs of STZ induced diabetic mice (STZ). (A-C) Detection of intracellular total biopterin, alkaline-stable oxidized biopterin (BH_2 plus biopterin) and BH_4 levels. (D-F) GTPCH1 protein expression was increased by fenofibrate treatment, while DHFR was unchanged. Values are mean ± SEM. n=6 per group. $^{*}P<0.05$, $^{**}P<0.01$ *vs* Control; $^{\#}P < 0.05$, $^{\#\#}P < 0.01$ *vs* STZ.

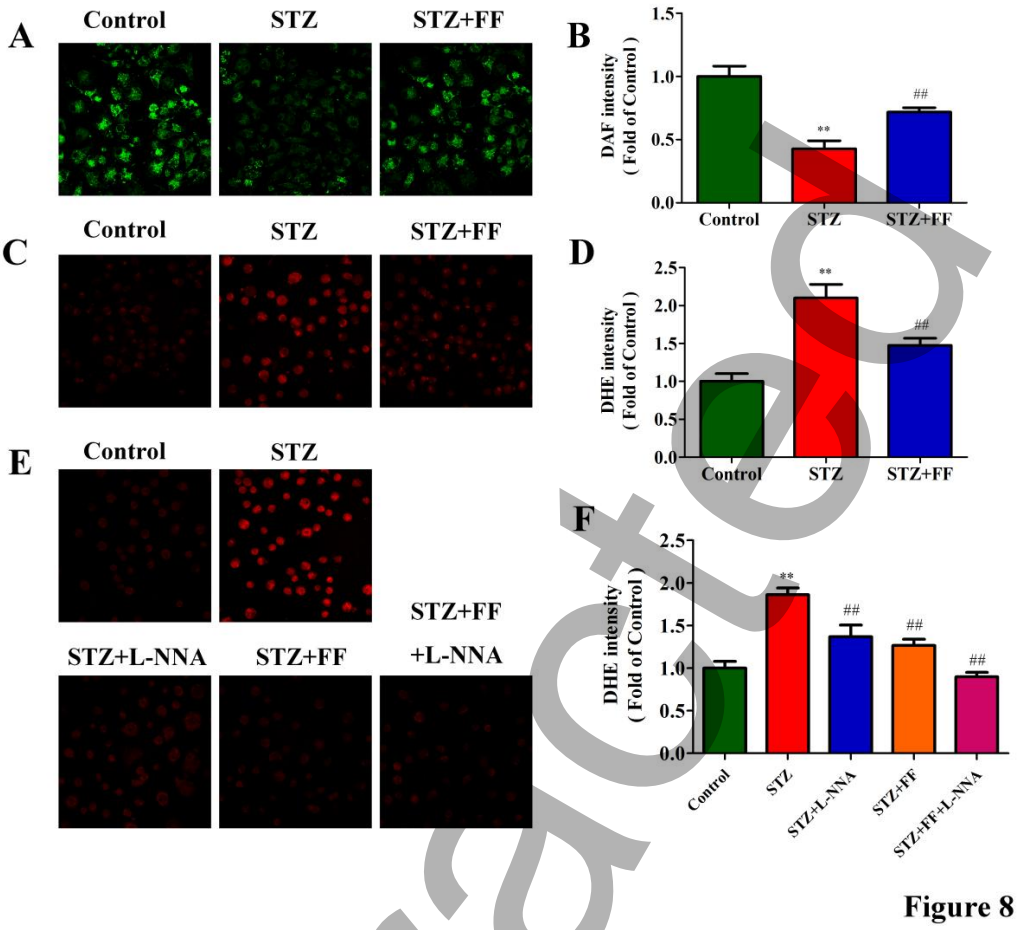

Figure 8

Figure 8. Fenofibrate (FF) prevented eNOS uncoupling in EPCs of STZ-induced diabetic mice (STZ). (A-D) Measurement of intracellular NO and O_2^- levels. (E and F) Determination of intracellular O_2^- production after incubation with NOS inhibitor L-NNA. Values are mean ± SEM. n=5-8 per group. $^{**}P<0.01$ *vs* Control; $^{\#\#}P < 0.01$ *vs* STZ.

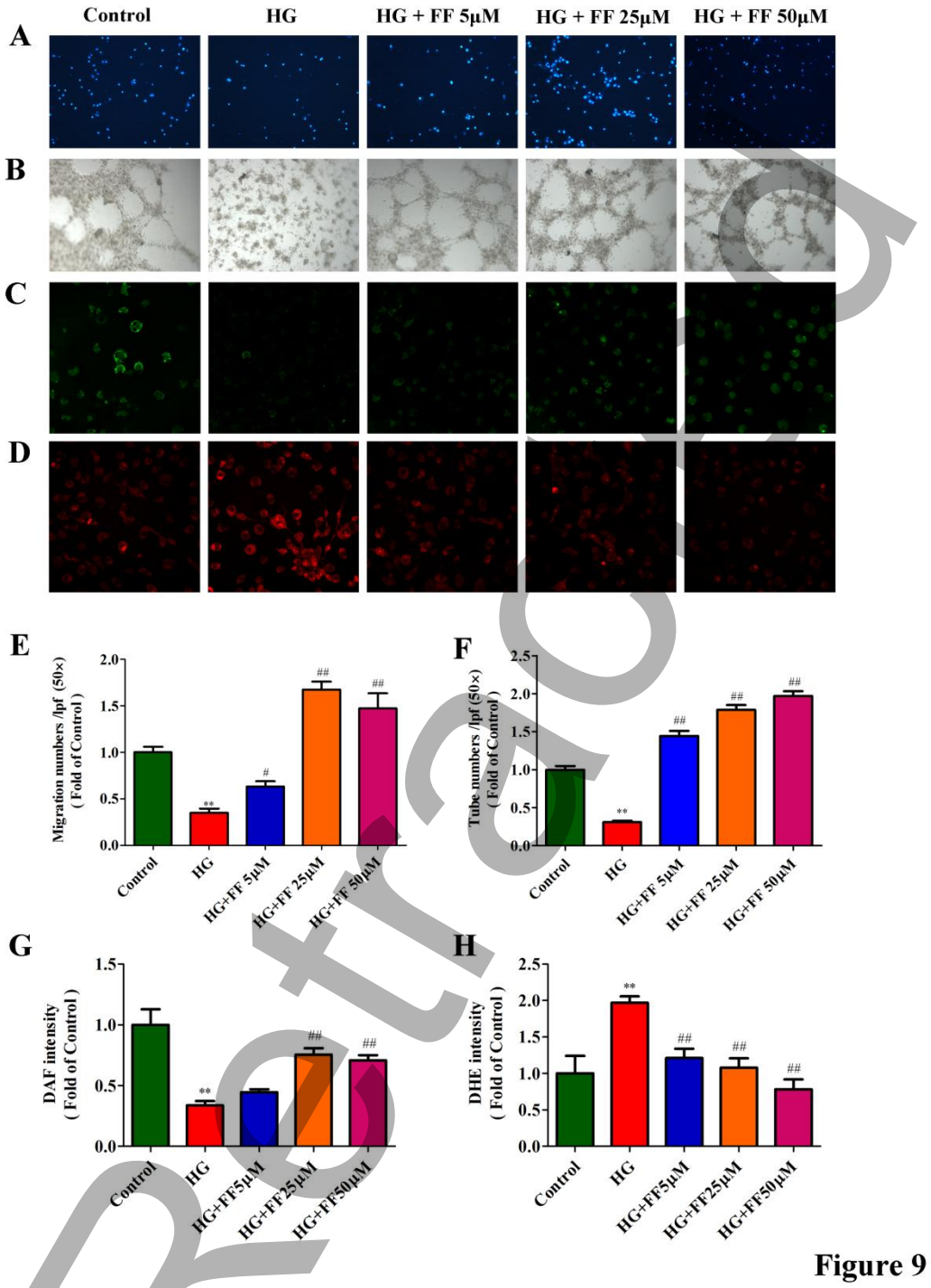

Figure 9

Figure 9. Fenofibrate (FF) improved impaired EPCs functions and prevented eNOS uncoupling of EPCs induced by high glucose (HG). EPCs from normal C57BL/6 mice were co-cultured with high glucose (33 mM) and fenofibrate (5, or 25, or 50 μM). Measurement of migratory capacity (A and E), tube formation ability (B and F), intracellular NO (C and G) and O_2^- (D and H) levels. Values are mean ± SEM. n=5-9 per group. $^{**}P<0.01$ *vs* Control; $^{\#}P < 0.05$, $^{\#\#}P < 0.01$ *vs* HG.